Colloid Polym Sci (2016) 294:1585–1598
DOI 10.1007/s00396-016-3920-9

ORIGINAL CONTRIBUTION

Selective adsorption and reusability behavior for Pb^{2+} and Cd^{2+} on chitosan/poly(ethylene glycol)/poly(acrylic acid) adsorbent prepared by glow-discharge electrolysis plasma

Jie Yu[1] · Jidong Zheng[1] · Quanfang Lu[1,2] · Shuxiu Yang[1] · Xiaomei Zhang[1] · Xing Wang[1] · Wu Yang[1]

Received: 28 April 2016 / Revised: 3 July 2016 / Accepted: 8 July 2016 / Published online: 23 July 2016

Abstract Using Pearson's hard and soft acids and bases (HSAB) principle as the design guideline, a novel chitosan/poly(ethylene glycol)/poly(acrylic acid) (CS/PEG/PAA) hydrogel adsorbent containing hard Lewis base adsorption site (i.e., amino group, hydroxyl group, ether linkage, carboxylate ions) was prepared by glow-discharge electrolysis plasma (GDEP) technique and then applied for the selective adsorption of Pb^{2+}. A copolymerization mechanism initiated by GDEP was proposed. The structure, thermal stability, and morphology of CS/PEG/PAA adsorbent were characterized by FT-IR, thermogravimetry/differential thermogravimetry (TG/DTG), and SEM. The effects of the solution pH and contact time on the single-component adsorption were examined by batch experiments. Competitive adsorptions of Pb^{2+} and Cd^{2+} were carried out under equal mass concentration and equal molar concentration. In addition, regeneration and reusability of adsorbent were also investigated in detail. The results showed that the maximum adsorption capacities for Pb^{2+} and Cd^{2+} are 431.7 and 265.0 mg g^{-1}, respectively. The kinetic behaviors of the adsorption and the fourth desorption for single component and the competitive adsorption for Pb^{2+} follow the pseudo-second-order model with pH = 4.8. The CS/PEG/PAA adsorbent has good adsorption selectivity for Pb^{2+} with the coexistence of Cd^{2+}. The adsorbent displays excellent regeneration and reusability in the EDTA-4Na solution.

Keywords Glow-discharge electrolysis plasma (GDEP) · Chitosan-based adsorbent · Adsorption kinetics · Desorption kinetics · Selective adsorption · Reusability

✉ Jie Yu
yujie741008@163.com

✉ Quanfang Lu
luqf@nwnu.edu.cn

[1] Key Lab of Bioelectrochemistry and Environmental Analysis of Gansu Province, College of Chemistry and Chemical Engineering, Northwest Normal University, Lanzhou 730070, People's Republic of China

[2] Editorial Department of the University Journal, Northwest Normal University, Lanzhou 730070, People's Republic of China

Introduction

Water pollution owing to the indiscriminate disposal of heavy metals has caused the extensive concern over the past few decades. Due to nondegradable and cumulative effects in living organisms, heavy metals bring the permanent contamination to the ecosystem, environment, and human health [1]. It is well known that heavy metals, especially lead (Pb^{2+}) and cadmium (Cd^{2+}), are generally found in industrial wastewater because of their wide applications in alloy industries, battery industries, paint pigments, metal plating, smelting, mining, and so on [2]. Lead can cause serious harmful effects on the reproductive system, liver and kidneys, immune system, and nervous system of human beings, especially children and infants even at very low concentrations. Cadmium can cause anemia and a yellow stain that gradually appears on the joints of the teeth. Therefore, effective removal of Pb^{2+} and Cd^{2+} from industrial wastewater will greatly help public health and environmental sustainability [1, 2]. Many methods, such as chemical precipitation, ion exchange, membrane separation, electrolysis, solvent extraction, and adsorption, have been developed for removal of Pb^{2+} and Cd^{2+} from industrial wastewater. Among them, the adsorption is one of the remarkable and economical methods because of its simplicity of design, ease of operation, and high efficiency [3–5].

In recent years, hydrogels with three-dimensional network structure and functional groups as adsorbents have received great attention for wastewater purification because of their high adsorption capacity and economic advantages [6–8]. However, most of the hydrogels are synthesized through petroleum chemical products. These adsorbents are of toxicity and nonbiodegradability; therefore, they can produce long-term and serious environmental issues [7, 8]. For these reasons, the development and application of biopolymer hydrogels have attracted great attention [9].

Chitosan (CS) is a naturally abundant and cheap polysaccharide with many useful characteristics, i.e., nontoxicity, biocompatibility, biodegradability, and antimicrobial ability [7, 9]. Owing to the reactivity of amine groups (the strong chelation properties for heavy metals) and hydroxyl groups, CS and its derivatives have been applied as promising adsorbents [10, 11]. However, the protonation of amino groups results in dissolution of CS in acidic solution, which limits CS to be used as an adsorbent in acidic media [7]. To overcome this drawback, the development of the eco-friendly chitosan-based hydrogels is one of the hot topics. Many methods, such as chemical initiation [12], grafting and crosslinking [13], chemical modification [14, 15], electrospinning [16], UV curing [17], irradiation [18], and glow-discharge electrolysis plasma (GDEP) [7], have been used to prepare chitosan-based hydrogels. Among these methods, GDEP technique has great potential because of its lower cost in setup, simple steps, mild reaction conditions, and temporal control over polymerization [7, 8]. GDEP is a kind of nonequilibrium plasma, which can produce various reactive chemical species such as HO·, H·, O·, HO_2·, and H_2O_2 in aqueous solution [19]. These active species can initiate the polymerization reaction [20–22]. This technique is also termed as a clean and environment-friendly source of initiation, which is not requiring any additional chemicals and leaving some unwanted residues. In addition, HO· radicals generated by GDEP in aqueous solutions can be linked to the polymer chains [7, 8, 21], so the hydrogel has better performance.

Over the past few decades, many studies have focused on the investigation of the adsorption kinetics, isotherms, and thermodynamics of adsorbents for various heavy metals. Nevertheless, the selectivity of adsorbent toward heavy metals is another focus of great research interest for water purification and resource recovery. Different approaches have been reported in the investigation of the adsorption selectivity. For example, Zhao et al. [11] studied EDTA and/or DTPA-functionalized chitosan as adsorbents (MEDCS/MDTCS) for the selectivity removal of Cd, Pb, Co, and Ni. Liu and Bai [23] examined the selective adsorption of Cu, Co, Ni, Zn, and Cd with DETA-functionalized PGMA adsorbent (P-DETA). Yantasee et al. [24] explored the selectivity of amine-functionalized activated carbon (NH_2–AC) toward Cd, Pb, Co, and Ni by comparing the distribution coefficient (K_d) of the heavy metals. However, most of these studies focused only on the selectivity of the amine-functionalized adsorbents. What is more, the preparation process of adsorbents is very complicated and can accomplish secondary pollution.

Recently, Koong et al. [25] found an important fact for designing selective adsorbents; that is, besides the inherent feature of functional groups, the organic matrix of the adsorbent plays an important role on the adsorption selectivity. Li et al. [26] found that both the characteristics of the functional groups on adsorbent and the properties of the heavy metals should be taken into consideration to account for the adsorption selectivity. Therefore, choosing appropriate monomers to synthesize selective adsorbent is very meaningful according to different needs. Irving-Williams order [27] and Pearson's hard and soft acids and bases (HSAB) principle [28, 29] are widely used to explain the stability of metal complexes and selective adsorption mechanism [26, 30]. On the contrary, Irving-Williams order and Pearson's HSAB principle may offer help to design selective adsorbents. Pearson classified every conceivable Lewis bases three categories, that is, hard, soft, or borderline, and proceeded to an equivalent classification of Lewis acids. According to the HSAB principle, the soft acids prefer to bind soft bases to give covalent complexes, whereas the hard acids prefer to bind the hard bases to give ionic complexes [28]. For example, Lam et al. [31] synthesized aminopropyl-containing MCM-41 adsorbent (NH_2–MCM-41) and then studied the selective separation of Ag^+ and Cu^{2+} by using the Pearson's HSAB principle. However, the adsorption selectivity cannot be predicted according to Pearson's HSAB principle when metals are considered the same category Lewis acid, such as Fe^{2+}, Co^{2+}, Ni^{2+}, Cu^{2+}, and Zn^{2+} (they are considered borderline Lewis acid). Irving and Williams [27] found that the stability of complexes for the first transition series followed the order $Mn^{2+} < Fe^{2+} < Co^{2+} < Ni^{2+} < Cu^{2+} > Zn^{2+}$. This order is just made up for a lack of first transition in the HSAB principle.

Selective adsorbent is usually a grafted and crosslinked copolymer, which has a very complicated structure. However, some functional groups of monomers may be changed or destroyed during the polymerization process. Therefore, designed selective adsorbents need to be tested by selective adsorption experiment. The effects of the solution pH [25, 32–34], metal ion concentration [25, 30, 32, 33], contact time [35], and metal percentage ratio [25] were examined on the selective adsorption process. Koong et al. [25] found that pH did not affect the adsorption selectivity; however, the adsorption capacity decreased with the solution pH and there was negligible adsorption at pH = 2 or even below. The adsorption isotherm data in binary metal mixture solution were evaluated using extended isotherm models [25, 32]. Clarification of the adsorption characteristics and kinetic behaviors of the adsorbent is necessary to design selective adsorption systems because kinetic model not only estimates the

adsorption rates, but also leads to how to express suitable reaction mechanism [30, 36]. However, there were few reports on the adsorption kinetic of adsorbent in binary metal mixture solution.

The regeneration is another important factor affecting an advanced adsorbent. Adsorbent possessing better reusability property will significantly reduce the overall cost [37]. Adsorption and desorption are widely used to investigate the possibility for the regeneration of the adsorbent [5]. In order to choose the optimum desorption conditions, the study of desorption kinetics is also really great and very meaningful. However, the kinetic behaviors of desorption were rarely studied [38].

Poly(ethylene glycol) (PEG) is a polymer of ethylene oxide with a general formula $HO(CH_2CH_2O)_nH$. It is a highly hydrophilic, nontoxic, biocompatible polymer [20]. Acrylic acid (AA) is the simplest unsaturated carboxylic acid [22]. In this work, the chitosan/poly(ethylene glycol)/poly(acrylic acid) (CS/PEG/PAA) adsorbent was synthesized in aqueous solution by a simple one step using the GDEP technique, in which *N*,*N*′-methylenebisacrylamide (MBA) was used as a crosslinking agent. The structure, thermal stability, and morphology of CS/PEG/PAA adsorbent were characterized by FT-IR, thermogravimetry/differential thermogravimetry (TG/DTG), and SEM. A grafted copolymerization mechanism initiated by GDEP was proposed. The effects of the solution pH and contact time on the single-component adsorption process were systematically examined by batch experiments. Competitive adsorption kinetic of Pb^{2+} with the coexistence of Cd^{2+} was carried out under equal mass ion concentration and equal molar concentration. In addition, reusability, desorption, and the fourth desorption kinetic behaviors of CS/PEG/PAA adsorbent were also investigated in detail.

Experimental

Materials

Chitosan (CS, 85 % degree of deacetylation) was supplied by Zhejiang Golden Shell Biological Chemistry Co., Ltd. *N*,*N*′-methylenebisacrylamide (MBA, CP) was used as a crosslinker. Acrylic acid (AA, AR) was distilled under reduced pressure before use. Poly(ethylene glycol) (PEG, M_n = 800), ethylenediaminetetraacetic acid tetrasodium salt (EDTA-4Na), $Pb(NO_3)_2$, $Cd(NO_3)_2{\cdot}4H_2O$, and HNO_3 were all of analytical grade.

Preparation of CS/PEG/PAA adsorbent

The experimental setup is similar to our previous work [22]. Into a 250-mL three-neck flask stirring for 20 min at 25 °C, 4 g PEG, 0.5 g CS, 0.03 g MBA, and 30 mL distilled water were added. Then, 7 mL AA was added into the above solution. After that, the mixture was raised to 75 °C and stirred for 10 min. After dissolving completely, two electrodes were immersed into the mixed solution to start the glow discharge at 630 V and 52 mA for 5 min. Then, the reaction mixture was stirred for an additional 4 h at 75 °C. And then, the product was neutralized the carboxylic groups of the grafted poly(-acrylic acid) by 0.1 mol L^{-1} NaOH solution to a degree of neutralization for about 80 %. Finally, the CS/PEG/PAA adsorbent was separated by filtration, washed several times with methanol, dried in a vacuum oven at 60 °C, and milled through a 100-mesh sieve.

Characterizations

The optical emission spectra produced by the GDEP in 200–1100 nm are measured by a multichannel optical fiber spectrometer (AvaSpec-2048-8). The thermal stability of CS/PEG/PAA adsorbent was determined by a PerkinElmer TG/DTA 6300 instrument. The structures of samples were recorded on a Digilab FTS3000 FT-IR spectrophotometer. Surface morphology of CS/PEG/PAA was observed on a field emission scanning electron microscope (ULTRA plus FESEM, Zeiss). The concentrations of Pb^{2+} and Cd^{2+} ions were measured three independent times by Varian 715-ES inductively coupled plasma-optical emission spectroscopy (ICP-OES) (Varian Inc.).

Property testing

Effect of pH on adsorption

The pHs ranging from 1.0 to 5.9 of the solution (300 mg L^{-1}) were adjusted with 0.1 mol L^{-1} HNO_3 solution. Into a conical flask, 0.03 g of adsorbent and 100 mL of the single metal ion solution (300 mg L^{-1}) were added. The mixtures were shaken with 140 r min^{-1} for 3 h at 25 °C. The adsorption capacity (Q_t) was calculated by the following:

$$Q_t = \frac{(C_0 - C_t)V}{m} \quad (1)$$

where Q_t (mg g^{-1}) is the adsorption capacity at time t, m (g) is the amount of adsorbent, C_0 and C_t (mg L^{-1}) are the concentrations of the metal ions at initial and time t, and V (L) is the volume of the solution.

Single- and binary-component adsorption kinetic

A 0.06-g adsorbent and 200-mL single heavy metals (300 mg L^{-1}, pH = 4.8) were added into the conical flask, and then, the mixtures were shaken with 140 r min^{-1} for 3 h at 25 °C. The binary-component adsorption kinetic was carried out using equal mass concentration (300 mg L^{-1}) and

equal molar concentration (1.45 mmol L^{-1}) with pH = 4.8. In this experiment, 0.06-g adsorbent was added into 200 mL of binary metal ion solution, shaken with 140 r min^{-1} at 25 °C, and measured at a certain interval. Heavy metal concentrations of a certain interval were determined by ICP-OES.

Reusability and desorption kinetics

A 0.03-g adsorbent was added into 100 mL of 300 mg L^{-1} (pH = 4.8) heavy metal solution and shaken with 140 r min^{-1} for 3 h at 25 °C. Then, after filtration, the solution was determined by ICP-OES and the adsorption capacity was calculated using Eq. (1). After that, the adsorbent loaded with heavy metals was put into the 100 mL of 0.015 mol L^{-1} EDTA-4Na solutions and shaken with 140 r min^{-1} for 3 h at 25 °C. The final metal ion concentrations were determined by ICP-OES. The desorption capacity $Q_{t,d}$ (mg g^{-1}) was calculated by Eq. (2).

$$Q_{t,d} = \frac{C_{t,d} V_d}{m} \tag{2}$$

where $Q_{t,d}$ (mg g^{-1}) is the desorption capacity, m (g) is the amount of adsorbent, $C_{t,d}$ (mg L^{-1}) is the concentration of desorption solution at time t, and V_d (L) is the volume of the desorption solution. The adsorbent was collected from the solution and washed with deionized water and then reused in the next adsorption process. Such adsorption-desorption cycles were repeated four times. The fourth desorption kinetic process was investigated. The desorption ratio (η) was given as follows [21]:

$$\eta = \frac{Q_d}{Q_a} \times 100\% \tag{3}$$

where η (%) is the desorption ratio, Q_d (mg g^{-1}) is the desorption capacity, and Q_a (mg g^{-1}) is the adsorption capacity.

Results and discussion

Polymerization mechanism of CS/PEG/PAA adsorbent initiated by GDEP

GDEP can give rise to active species, electron beam radiation, shock waves, and ultraviolet light in aqueous solution. Normally, the GDEP can generate 5–20 eV energetic electrons [39]. Excitation and ionization of H_2O molecules by these energetic electrons lead to breaking bonds of H_2O molecular and then to production of reactive species, such as HO·, H·, and O· radicals, and H_2O_2, H_2, and O_2 molecular, among which HO· is one of the strongest oxidants with a standard oxidation potential ($E^0_{HO\cdot/H2O}$) of 2.85 V [40, 41]. Figure 1 shows that the typical emission spectrum produced HO·, H·, and O· by the GDEP in 200–1100 nm for the mixed solution of CS, PEG, and AA at 630 V (inset is the photograph of the GDEP at 630 V). Bands at 283.0 and 309.2 nm are attributed to the emission of HO· radicals ($A^{2+} \rightarrow X^2\Pi$) ((1, 0) and (0, 0), respectively). The peaks at 486.1 and 656.2 nm are assigned to the atomic hydrogen emission lines (H_β (4d $^2D \rightarrow 2p\ ^2P^0$) and H_α (3d $^2D \rightarrow 2p\ ^2P^0$), respectively). In addition, emission lines of atomic oxygen (O (3p $^5P \rightarrow 3s\ ^5S^0$) at 777.1 nm and O (3p $^3P \rightarrow 3s\ ^3S^0$) at 844.6 nm) are found in the near-infrared region [42, 43]. The Na emission line is also produced at 589.6 nm in the spectra, suggesting that it comes from the mixed solution.

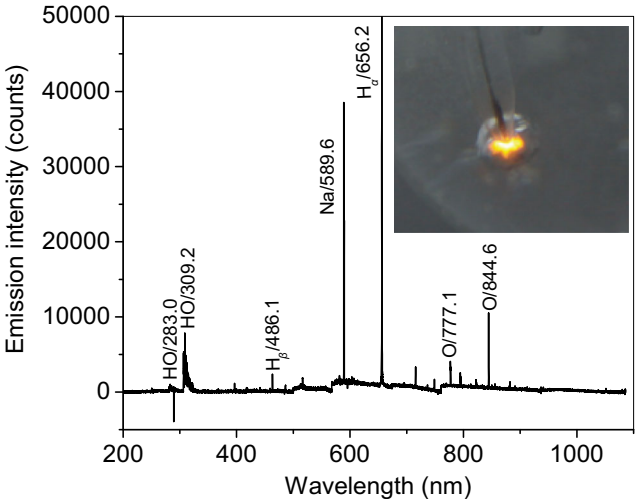

Fig. 1 Typical emission spectrum from the GDEP in the mixed solution of CS, PEG, and AA at applied voltage of 630 V (*inset* is the photograph of GDEP at 630 V)

The reaction mechanism of GDEP may be similar to those in radiation and photochemical processes, which produce radicals and molecular through excitation and ionization. Therefore, the important reaction mechanism by GDEP is assumed as follows [44]:

$$H_2O + e^* \rightarrow HO\cdot + H\cdot \quad \text{dissociation}$$
$$H_2O + e^* \rightarrow O\cdot + H_2 \quad \text{dissociation}$$
$$HO\cdot + HO\cdot \rightarrow H_2O_2$$
$$HO\cdot + HO\cdot \rightarrow H_2O + O\cdot$$
$$O\cdot + HO\cdot \rightarrow O_2 + H\cdot$$
$$HO\cdot + H_2O_2 \rightarrow HO_2\cdot + H_2O$$
$$H\cdot + H\cdot \rightarrow H_2$$
$$HO\cdot + HO_2\cdot \rightarrow H_2O + O_2$$

where * indicates a high-energy state. The unique characteristic of GDEP is their strong deviation from the yield expected according to Faraday's law [45]. Further, the products, such as radicals (HO·, H·, O·, and HO_2·) and molecules (H_2, H_2O_2, and O_2), are novel for normal electrolysis. HO· radicals directly attack organic compounds leading to the three different classes [40, 44, 45].

1. Abstraction of hydrogen atom. Under the condition of saturated aliphatic hydrocarbons and alcohols, HO· will react primarily by organic abatement to yield water and an organic radical (R·):

$$HO\cdot + RH \rightarrow H_2O + R\cdot$$

2. Electrophilic addition to unsaturated bond. Addition reactions usually take place with unsaturated aliphatic and aromatic compounds. In the case of alkene hydrocarbons, HO· radical will add to unsaturated double C=C bonds of organic compound forming a C-centered radical with a hydroxyl group at the α-C atom:

$$HO\cdot + R_2C = CR_2 \rightarrow R_2(OH)C{-}CR_2\cdot$$

3. Electron transfer. If hydrogen abstraction or electrophilic addition reaction is disfavored by multiple halogen substitution or steric hindrance, the reduction of hydroxyl radicals to hydroxide anions by an organic substrate may be occurred:

$$HO\cdot + RX \rightarrow XR\cdot^{+} + OH^{-}$$

Moreover, H· radicals are strong reducing agents ($E^0_{H2O/H\cdot} = -2.30$ V). In the presence of organic compounds, H· radicals will go through two general types of reactions [41, 45]: (i) hydrogen abstraction from saturated compounds and (ii) hydrogen addition to unsaturated. The two reactions of H· radicals often follow the same mechanism as those of HO· radicals.

Thus, in the initiated copolymerization of CS, PEG, and AA using GDEP, reactions of the hydrogen abstraction from CS and PEG and the electrophilic addition of AA are simultaneously present. The proposed copolymerization mechanism of the prepared CS/PEG/PAA by GDEP is shown in Scheme 1. At first, H_2O molecules can be dissociated into HO·, H·, and O· radicals by the energetic electrons from GDEP, which is called the radical-forming process (reaction (1)). Then, HO· will react with labile H atoms from CS and PEG by abstraction of hydrogen to form water and the new organic radical (a and b). Meanwhile, HO· radicals will also add to unsaturated double C=C bonds of AA forming the new organic radicals (c). The above reactions are called the chain initiation process (reaction (2)). After that, these organic radicals (a, b, and c) optionally react with the CS, PEG, and AA monomers to produce macromolecule free radicals (d, e, and f) and lead to the chain propagation (reaction 3). In the process of reaction 3, different types of radical species are simultaneously present. However, degradation of organic compounds by HO· is ignored due to the formation of copolymer to cease from further reaction if discharge conditions, i.e., applied voltage and discharge time, are controlled appropriately. Finally, reactions of macromolecule radicals are terminated by crosslinking copolymerization of crosslinking agent MBA, radical-radical combinations, and disproportionations to form a three-dimensional network copolymer [7, 8, 20, 21], which is called the termination reaction. And then, copolymers are neutralized the –COOH of the grafted poly(acrylic acid) by NaOH solution. After that, the resulting product is obtained (reaction 4). So, we can say that copolymerization mechanism initiated by GDEP is a free radical addition-crosslinking reaction. Finally, the CS/PEG/PAA hydrogel adsorbent is applied for the adsorption of Pb^{2+} and Cd^{2+}. It is found that the adsorbent has good adsorption selectivity for Pb^{2+} with the coexistence of Cd^{2+} (reaction 5).

Characterization of CS/PEG/PAA adsorbent

FT-IR analysis

The FT-IR spectra of the CS (a), PEG (b), AA (c), and CS/PEG/PAA adsorbent (d) are shown in Fig. 2. As can be seen from Fig. 2, the main characteristic peaks of CS (a) are at 3445 cm^{-1} (N–H and O–H stretch), 1659 cm^{-1} (C=O of amide bend), 1600 cm^{-1} ($-NH_2$ bend), 1325 cm^{-1} (C–N stretch), and 1156 cm^{-1} (bridge O stretch) [7]. The main characteristic peaks of PEG (b) are at 3405 cm^{-1} (O–H stretch), 2890 cm^{-1} (C–H stretch), and 1116 cm^{-1} (C–O–C stretch) [20]. The main characteristic peaks of AA (c) are at 1706 cm^{-1} (C=O stretch) and 1632 cm^{-1} (C=C stretch) [20]. In the spectra of adsorbent (Fig. 2 (d)), the peaks at 1600 cm^{-1} ($-NH_2$ bend) of CS and 1632 cm^{-1} (C=C stretch) of AA disappear completely. Moreover, some new peaks at 1560 and 1453 cm^{-1} (C=O of $-COO^-$ asymmetric [7, 8] and symmetric stretch), which are corresponded to be neutralized –COOH groups, and 1116 cm^{-1} (C–O–C stretch) appear. All above information suggested that PEG and AA have been grafted onto the CS backbone forming copolymers by GDEP.

TG/DTG analysis

TG and DTG have been applied as a powerful thermo analytical technique to monitor physical and chemical changes in both natural and synthetic polymers [46]. Figure 3 shows the TG (a) and DTG (b) curves of CS and CS/PEG/PAA absorbent. It is obvious that CS has two main weight loss stages. The first step at 25 to 148 °C is ascribed to the loss of the absorbed/bound moisture [47] and corresponded to weight

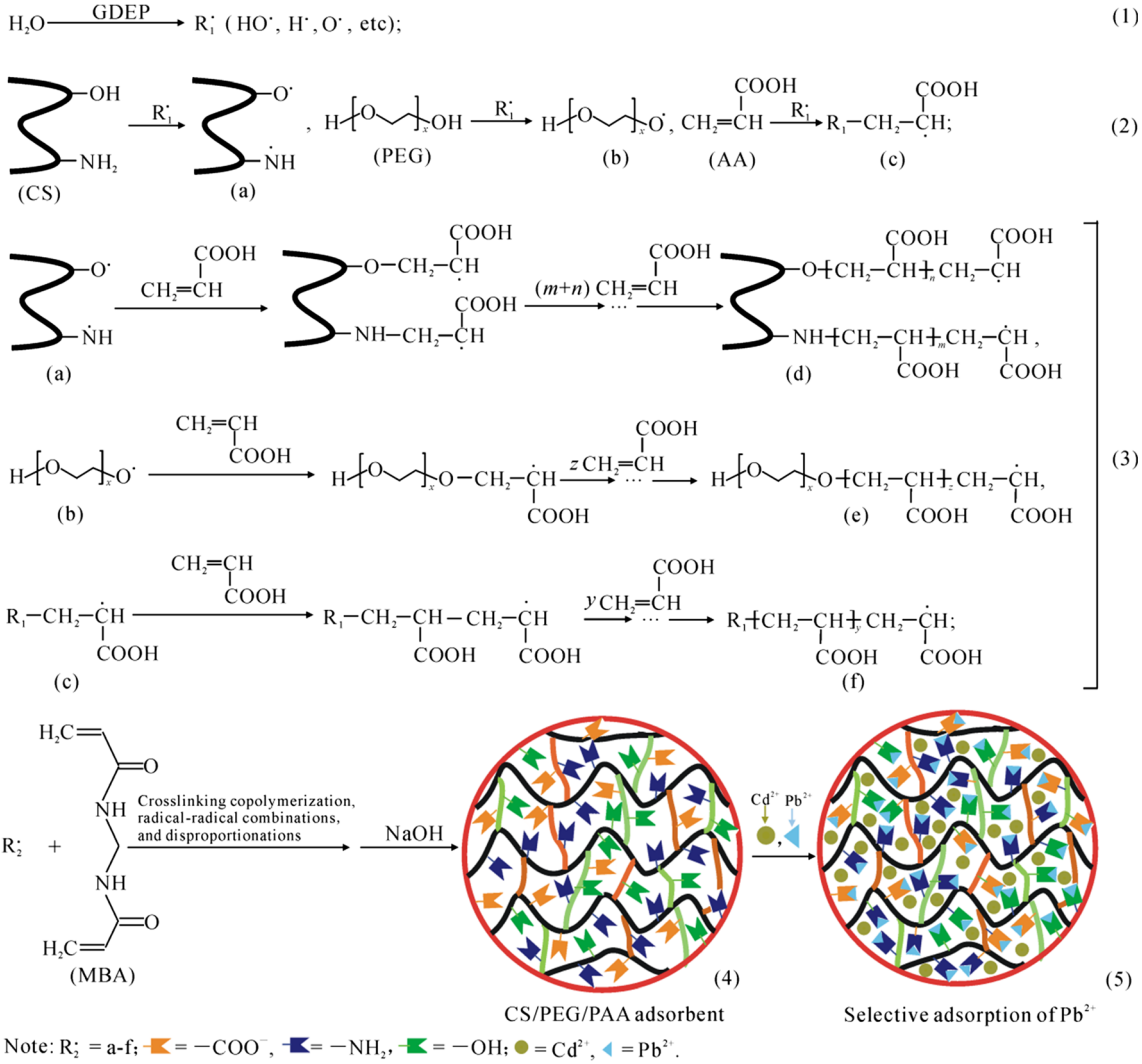

Scheme 1 Copolymerization mechanism of CS/PEG/PAA initiated by GDEP. (*1*) radical formation, (*2*) chain initiation, (*3*) chain propagation, (*4*) chain termination and neutralization of acrylic acid, and (*5*) selective adsorption of Pb^{2+} with the coexistence of Cd^{2+}

loss of 6.2 %. The second weight loss of 45 % from 148 to 390 °C is attributed to decomposition of main chain C–C bond of CS. However, the CS/PEG/PAA adsorbent has three steps for continuous thermal decomposition. Weight loss of 20 % from 25 to 340 °C is attributed to the removal of absorbed/bonded water and the decomposition of low polymer and non-grafted CS. The two weight losses of about 16 % from 340 to 420 °C are ascribed to the decomposition of grafted CS. The third weight loss of about 29.2 % from 400 to 520 °C is ascribed to the breakage of crosslinking network structure and the decomposition of grafted poly(acrylic acid) (PAA) and PEG chain in the polymeric backbone. The total weight losses of CS and CS/PEG/PAA are 65.4 and 60.2 % at about 800 °C. Clearly, CS/PEG/PAA adsorbent has a higher decomposition temperature than CS.

The DTG curves of CS and CS/PEG/PAA are shown in Fig. 3b. The maximum degradation temperature (T_{max}) of CS is at 300 °C. However, the T_{max} of CS/PEG/PAA is at 390 and 448 °C. All results showed that grafted PEG and AA onto CS can enhance the thermal stability of the CS. This further indicated that the CS/PEG/PAA absorbent presents high thermal stability.

SEM analysis

The microstructure morphology of the CS/PEG/PAA absorbent after being freeze-dried was observed at two different magnifications as shown in Fig. 4. The adsorbent shows a rough surface and a network structure with many pores. The unique sponge-like structure can increase the area of contact with the solution, facilitate heavy metals to diffuse into the three-dimensional network, improve the adsorption capacity, and accelerate the adsorption rate [7, 8].

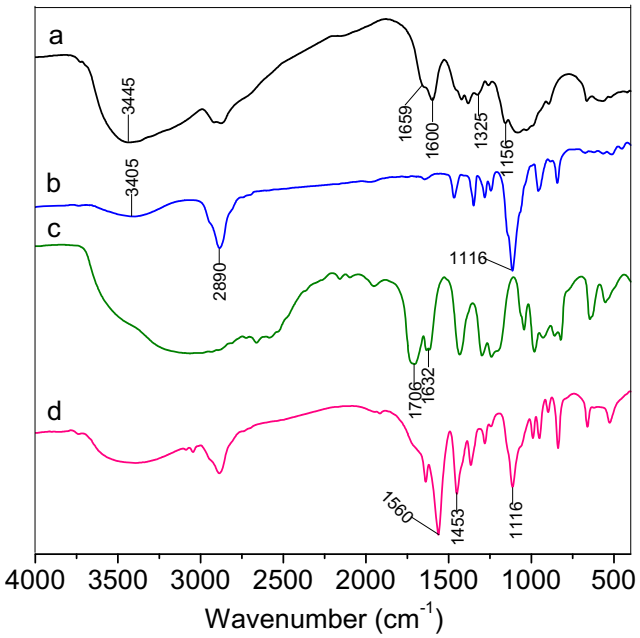

Fig. 2 FT-IR spectra of CS (*a*), PEG (*b*), AA (*c*), and CS/PEG/PAA adsorbent (*d*)

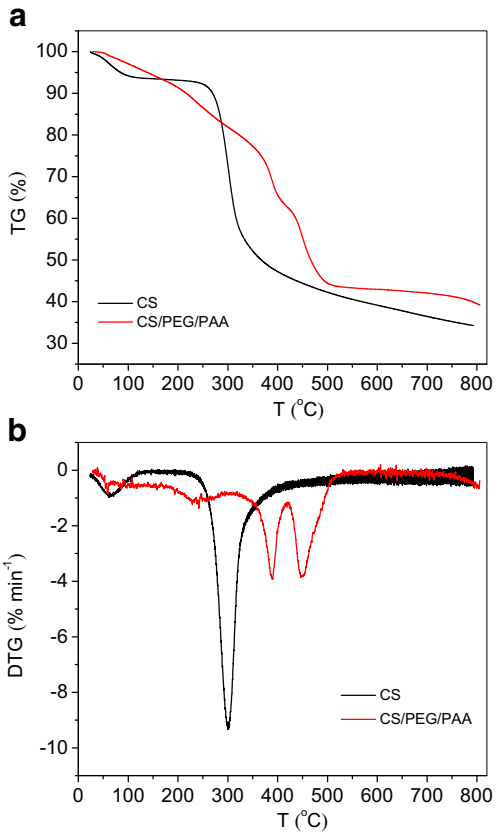

Fig. 3 TG (**a**) and DTG (**b**) curves of CS and CS/PEG/PAA adsorbent

Adsorption of CS/PEG/PAA for single component

Effect of pH on adsorption

The pH of solutions not only affects the protonation degree and surface charge of the adsorbent, but also influences the speciation of the heavy metal ions [48]. The adsorption of Pb^{2+} and Cd^{2+} on CS/PEG/PAA was investigated at pH = 1.0–5.9 because Pb^{2+} and Cd^{2+} ions could be precipitated by OH^- to form metal hydroxide above pH 5.9. Figure 5 shows the effect of pH on single component of Pb^{2+} and Cd^{2+} adsorption. The adsorption capacities of Pb^{2+} and Cd^{2+} increase at pH = 2–4.8 and then slightly decrease with the increase of pH. Therefore, we chose pH = 4.8 as the optimum pH of adsorption.

At lower pH (pH < 2), the competition from H^+ ions and the protonation can affect adsorption sites (amino group, hydroxyl group, ether linkage, carboxylate ions), which may block the chelation interaction between these groups and heavy metals [49]. Moreover, the adsorbent is in a collapsed and shrunken state. As a result, it is difficult for heavy metal ions to diffuse into the interior of adsorbent, and so, the adsorption capacity is very low [20]. With increasing the pH from 2.0 to 4.8, the competition from H^+ ions is weakened and the protonation degree of adsorption groups is decreased [50]. So, the heavy metal ions can easily be diffused into the polymeric network, the interactions of ion exchange and chelation can significantly be increased, and the adsorption capacity is improved. Further increase of pH from 4.8 to 5.9, the higher pH may cause the combination or precipitation between metal ions and hydroxide ions and bring adverse effects on adsorption [49].

Single-component adsorption kinetics

Figure 6 shows the adsorption kinetics of the single-component Pb^{2+} and Cd^{2+} on CS/PEG/PAA adsorbent at 25 °C. It is observed that the Pb^{2+} adsorption capacities increase sharply within 30 min, after that, continue to increase with a slower rate between 30 and 50 min, and finally level off after 60 min. However, Cd^{2+} adsorption capacities increase sharply within 10 min, then become slowly from 10 to 50 min, and finally level off after 60 min. The equilibrium adsorption capacities of Pb^{2+} and Cd^{2+} are 431.7 and 265.0 mg g^{-1}, respectively, implying that CS/PEG/PAA has high adsorption capacities and quite fast adsorption rate. The initial fast adsorption rate is due to the availability of many adsorption sites near the metal ions. With the proceeding of adsorption, the available sites and the adsorption rates decrease [51]. The possible explanation of the above is the different ionic radii of metals (Cd^{2+} 109 pm; Pb^{2+} 133 pm). Cd^{2+} ions can move quickly in the solution and interact with the functional groups of CS/PEG/PAA adsorbent because of the smaller size. However, Pb^{2+} ions are larger, making their

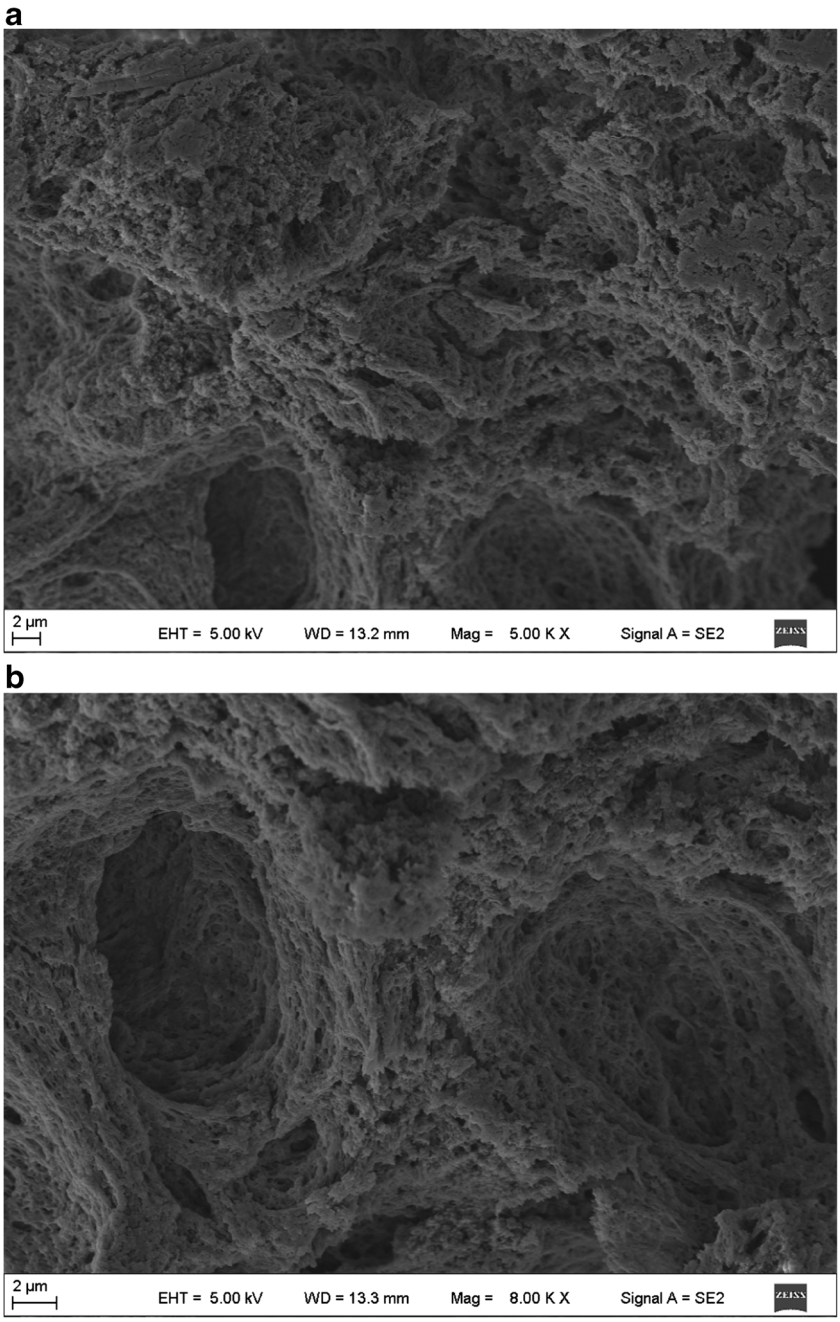

Fig. 4 SEM of CS/PEG/PAA adsorbent at different magnifications (**a** ×5000, **b** ×8000)

mobility in the solutions more difficult. Therefore, the diffusion of Pb^{2+} ions onto CS/PEG/PAA adsorbent is slower [13].

In order to investigate the adsorption mechanism, the pseudo-first-order and the pseudo-second-order kinetic models are commonly applied to evaluate the kinetic experimental data [51]. The pseudo-first-order kinetic equation is assumed that the adsorption is originated from physical process. It is given as follows:

$$\log(Q_e - Q_t) = \log Q_e - \frac{k_1}{2.303} t \tag{4}$$

where k_1 (min^{-1}) is the adsorption rate constant and Q_e and Q_t (mg g^{-1}) are the adsorption capacities at equilibrium and at time t (min), respectively. The intercept ($\log Q_e$) and slope ($-k_1/2.303$) of $\log(Q_e - Q_t)$ versus t (Fig. 7a) are used to calculate the parameters of Q_e and k_1 (Table 1).

The pseudo-second-order kinetic model is in agreement with the chemisorption mechanism being the rate-controlling step [7, 8]. It is given as follows:

$$\frac{t}{Q_t} = \frac{1}{k_2 Q_e^2} + \frac{t}{Q_e} \tag{5}$$

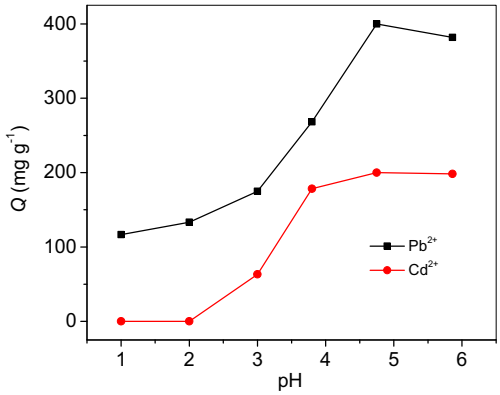

Fig. 5 Effect of pH on single adsorption of Pb^{2+} and Cd^{2+} (C_0 = 300 mg L^{-1}, V = 100 mL, m = 0.03 g, t = 180 min)

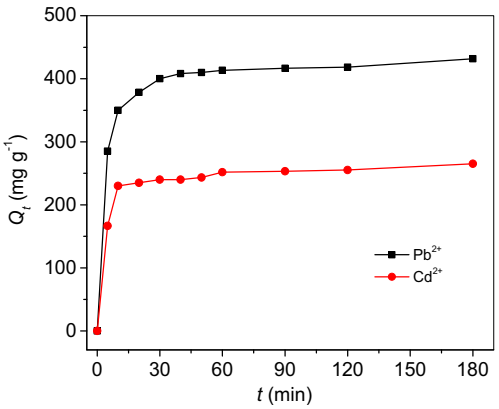

Fig. 6 Adsorption kinetics of Pb^{2+} and Cd^{2+} in single-component solution (C_0 = 300 mg L^{-1}, V = 200 mL, pH = 4.8, m = 0.06 g)

where k_2 (g mg^{-1} min^{-1}) is the rate constant of the pseudo-second-order model. The intercept ($1/k_2Q_e^2$) and slope ($1/Q_e$) of t/Q_t versus t (Fig. 7b) are used to calculate the parameters of k_2 and Q_e (Table 1).

Figure 7 shows the pseudo-first-order (a) and pseudo-second-order (b) kinetic model of Pb^{2+} and Cd^{2+} on CS/PEG/PAA adsorbent. By comparing Fig. 7a, b, it is obvious that pseudo-second-order model agrees with the experimental data better than the pseudo-first-order model. The R^2 and Q_e are frequently used to evaluate adaptability of two kinetic models. As can be seen from Table 1, the R^2 values of the pseudo-second-order model are closer to unity 1 and higher than those of the pseudo-first-order kinetics. Moreover, the Q_e values (Pb^{2+} 434.8 mg g^{-1} and Cd^{2+} 266.7 mg g^{-1}) obtained from the pseudo-second-order model are closer to the experimental $Q_{e,exp.}$ values (Pb^{2+} 431.7 mg g^{-1} and Cd^{2+} 265.0 mg g^{-1}) than those from the pseudo-first-order kinetic Q_e values (Pb^{2+} 115.7 mg g^{-1} and Cd^{2+} 73.7 mg g^{-1}). All these results suggested that the adsorption kinetics of Pb^{2+} and Cd^{2+} fits well to the pseudo-second-order model. So, the rate-limiting step in the adsorption process of Pb^{2+} and Cd^{2+} onto CS/PEG/PAA might be a chemisorption process [22].

The adsorption capacities of Pb^{2+} and Cd^{2+} ions on CS/PEG/PAA adsorbent synthesized by GDEP were quantitatively compared with other chitosan-based absorbents, which were obtained by other techniques and are listed in Table 2. The results showed that the CS/PEG/PAA adsorbent has higher adsorption capacities. It suggested that CS/PEG/PAA adsorbent has promising performance for the removal of Pb^{2+} and Cd^{2+} ions from aqueous solution. The higher adsorption capacities indicated once again that the GDEP technique has great potential for preparation of chitosan-based adsorbents. This technique can be considered as a rich source of free radicals in aqueous solution and applied to induce the polymerization reaction. Compared with other initiation techniques in Table 2, GDEP has low cost, mild reactive condition, controllable reaction, and no secondary pollution. Moreover, HO· radicals produced by GDEP can be added to the polymer chains, so the CS/PEG/PAA adsorbent has promising properties [20, 21].

Binary-component adsorption kinetics and selectivity

Figure 8 shows the kinetic curves of the binary components of Pb^{2+} and Cd^{2+} on CS/PEG/PAA adsorbent with equal mass concentration of 300 mg L^{-1} (Fig. 8a) and equal molar

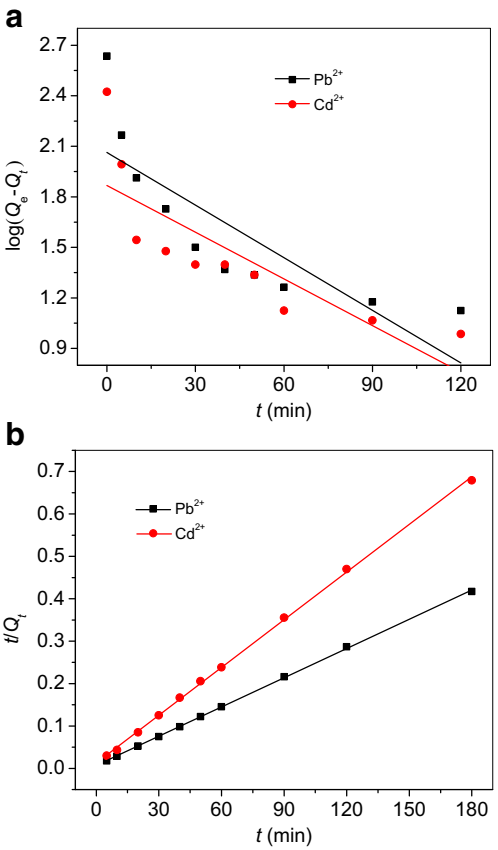

Fig. 7 Pseudo-first-order kinetic model (**a**) and pseudo-second-order kinetic model (**b**) of Pb^{2+} and Cd^{2+} on CS/PEG/PAA adsorbent (C_0 = 300 mg L^{-1}, V = 200 mL, pH = 4.8, m = 0.06 g)

Table 1 Kinetic parameters for adsorption of Pb^{2+} and Cd^{2+} on CS/PEG/PAA absorbent at pH = 4.8 with 25 °C

Metal ions	$Q_{e,exp.}$ (mg g^{-1})	Pseudo-first-order model		Pseudo-second-order model			
		k_1 (min^{-1})	Q_e (mg g^{-1})	R^2	$k_2 \times 10^{-4}$ (g mg^{-1} min^{-1})	Q_e (mg g^{-1})	R^2
Pb^{2+}	431.7	0.024	115.7	0.6433	7.83	434.8	0.9997
Cd^{2+}	265.0	0.0213	73.3	0.6276	10.81	266.7	0.9993

concentrations of 1.45 mmol L^{-1} (i.e., 300 mg L^{-1} Pb^{2+} and 163 mg L^{-1} Cd^{2+}) (Fig. 8b). It is shown from Fig. 8 that the adsorption capacity of Cd^{2+} ions increased sharply at initial 10 min, then decreased gradually from 10 to 50 min, and finally became almost negligible after 180 min. Obviously, the initially adsorbed Cd^{2+} ions on CS/PEG/PAA adsorbent were subsequently released into the solution in the binary-component adsorption process. However, the adsorption capacity of Pb^{2+} is increased until 180 min in 300 mg L^{-1} equal mass concentration system (Fig. 8a) and the adsorption capacity of Pb^{2+} is first increased and then reached equilibrium after 60 min in 1.45 mmol L^{-1} equal molar concentration system (Fig. 8b). The explanation of this result is the different metal ion ratio due to different molar mass (112.4 g mol^{-1} for Cd^{2+} and 207.2 g mol^{-1} for Pb^{2+}). The metal ion ratios of Cd^{2+}/Pb^{2+} are 2.67:1.45 and 1.45:1.45 in equal mass concentration and equal molar concentration system, respectively.

The adsorption data of Pb^{2+} ions were also fitted with the pseudo-second-order kinetic model (inset in Fig. 8). The kinetic parameters for adsorption of Pb^{2+} on CS/PEG/PAA absorbent in binary-component solution are listed in Table 3. It is observed from Table 3 and inset in Fig. 8 that the adsorption kinetics of Pb^{2+} ions also fit well to the pseudo-second-order model in binary-component solution.

The distribution coefficients K_d (mL g^{-1}) and selectivity coefficient α can be used to reflect the stability of a metal-ligand complex. The higher the K_d and α value are, the more stable the metal-ligand complex is. The high K_d and α values of metal ions are favorable also because they indicate the high affinity of the adsorbent to that of the metal ions [24]. The K_d and α can be expressed as follows [24, 52]:

$$K_d = \frac{C_0 - C_e}{C_e} \times \frac{V}{m} \tag{6}$$

$$\alpha = \frac{K_d(Pb^{2+})}{K_d(Cd^{2+})} \tag{7}$$

where C_0 and C_e (mg L^{-1}) are the concentrations of metal ions before and after adsorption, respectively, V (L) is the volume of solution, and m (g) is the mass of adsorbent. Table 4 lists the K_d and α of Pb^{2+} and Cd^{2+} on CS/PEG/PAA adsorbent at different initial concentrations. As can be seen from Table 4, the K_d values of Pb^{2+} are much higher than those of Cd^{2+}. The values of α are 30.2 and 24.5. So, we can say that the CS/PEG/

Table 2 Comparison of adsorption capacities for Pb^{2+} and Cd^{2+} based on chitosan adsorbents

Adsorbent	Preparing method	Q (mg g^{-1})		Refs
		Pb^{2+}	Cd^{2+}	
PVA/CS bead	IPN and crosslinking	166.4	126.1	[3]
Silica gel/chitosan composite	Sol-gel method	316.0	–	[4]
CS crosslinked with ECH-TPP	Phase inversion	166.9	83.75	[5]
Pristine CS	–	238.4	96.7	[10]
Magnetic EDTA-chitosan	Emulsion crosslinking	213.4	168.5	[11]
Magnetic DTPA-chitosan	Emulsion crosslinking	181.9	175.5	[11]
CS-co-MMB-co-PAA hydrogel	Chemical initiation	163.9	135.5	[12]
CS crosslinked with GA	Schiff's base	113.0	124.0	[13]
CS crosslinked with ECH	Crosslinking	107.0	92.0	[13]
CS-g-IA crosslinked with GA	Grafted crosslinking	334.0	405.0	[13]
CS-g-IA crosslinked with ECH	Grafted crosslinking	297.0	331.0	[13]
EGTA-modified chitosan	Chemical modification	103.6	83.18	[14]
Modified CS	Chemical modification	418.5	31.47	[15]
PEO/CS membrane	Electrospinning	214.8	232.3	[16]
CS/PEG/PAA adsorbent	GDEP technique	431.7	265.0	This work

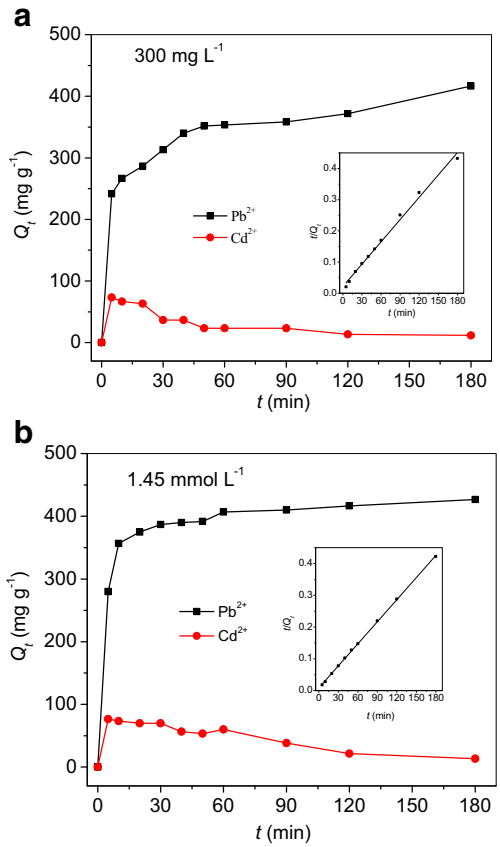

Fig. 8 Adsorption kinetics of Pb^{2+} and Cd^{2+} in binary component solution at V = 200 mL, pH = 4.8, and m = 0.06 g (**a** 300 mg L^{-1}, **b** 1.45 mmol L^{-1})

PAA adsorbent has good adsorption selectivity for Pb^{2+} with the coexistence of Cd^{2+}.

Both the characteristics of the functional groups on CS/PEG/PAA and the properties of the metal ions should be taken into consideration to account for the adsorption selectivity. According to the hard and soft acids and bases (HSAB) principle [28, 29], Pb^{2+} is considered a borderline Lewis acid, while Cd^{2+} is considered a Lewis soft acid. In addition, adsorption sites (amino group, hydroxyl group, ether linkage, carboxylate ions) of CS/PEG/PAA adsorbent are all considered hard base. The rule of HSAB principle is the following: Hard acids prefer to bind the hard bases and soft acids prefer to bind the soft bases [29]. It suggested that the coordination bonds between chelating group

Table 3 Kinetic parameters for adsorption of Pb^{2+} on CS/PEG/PAA absorbent in binary component solution

Concentration	$Q_{e,exp.}$ (mg g^{-1})	k_2 ($\times 10^{-4}$) (g mg^{-1} min^{-1})	Q_e (mg g^{-1})	R^2
300 mg/L Pb^{2+} and Cd^{2+}	416.7	2.66	418.4	0.9924
1.45 mmol/L Pb^{2+} and Cd^{2+}	426.7	6.61	431.0	0.9996

Table 4 The distribution coefficient K_d (mL g^{-1}) and selectivity coefficient α for Pb^{2+} and Cd^{2+} on CS/PEG/PAA adsorbent at different initial concentrations

Concentrations	K_d (mL g^{-1})		α
	Pb^{2+}	Cd^{2+}	
300 mg L^{-1} Cd^{2+} and Pb^{2+}	2302.03	76.13	30.2
1.45 mmol L^{-1} Cd^{2+} and Pb^{2+}	1867.95	76.41	24.5

and Pb^{2+} are more stable than those of Cd^{2+}. When the adsorbent was added into the mixture solution, all metal ions had the opportunities to occupy the chelating sites because a large number of unreacted chelating groups existed in adsorbent. When the chelating sites were occupied by adsorbed metal ions, no metal ions could diffuse toward the adsorption sites except Pb^{2+}. The result suggested that the coordination bonds between chelating group and Pb^{2+} are more stable than those of Cd^{2+}. When the Pb^{2+} ions were diffused into the chelating sites of adsorbent, they could replace Cd^{2+} of adsorbed [53]. Therefore, the adsorption capacity of Pb^{2+} is gradually increased over time, and the adsorption capacity of Cd^{2+} is increased first and then decreased over

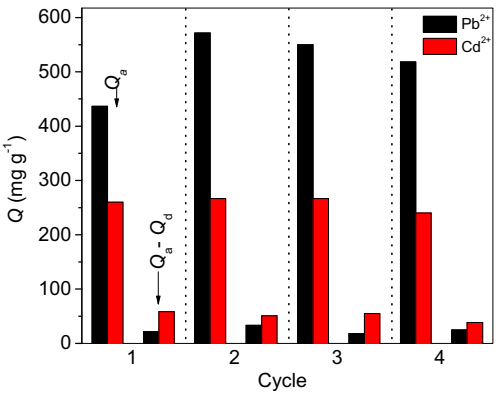

Fig. 9 Adsorption capacities of Pb^{2+} and Cd^{2+} at sequential four adsorption-desorption cycles using 0.015 mol L^{-1} EDTA-4Na as eluent

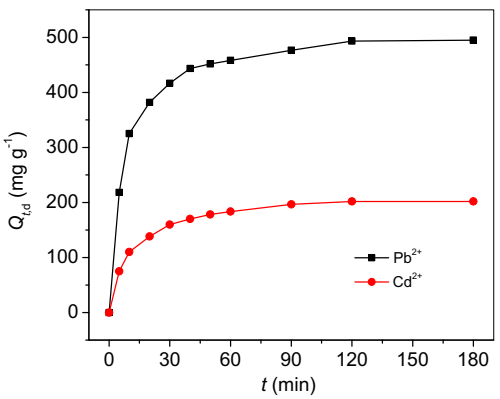

Fig. 10 The fourth desorption kinetics of Pb^{2+} and Cd^{2+} in 0.015 mol L^{-1} EDTA-4Na solution

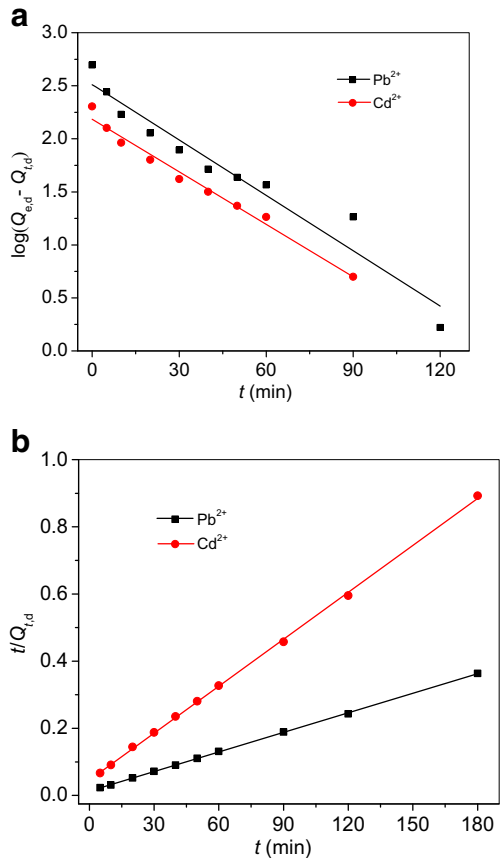

Fig. 11 Pseudo-first-order (**a**) and pseudo-second-order (**b**) desorption kinetic models of Pb^{2+} and Cd^{2+}

time until zero. That is, the CS/PEG/PAA adsorbent has outstanding selective adsorption for Pb^{2+} after a proper adsorption time.

Reusability and desorption kinetics

Adsorption and desorption are very important to study the regeneration of the adsorbent [5, 21]. Figure 9 shows the reuse potential of the CS/PEG/PAA absorbent via four times of adsorption and desorption experimental using 0.015 mol L^{-1} EDTA-4Na as eluent. In the adsorption process, the adsorption capacity of Cd^{2+} nearly remained a constant and the adsorption capacity of Pb^{2+} was higher than that of the first cycle. After desorption, remained Pb^{2+} and Cd^{2+} ions on the adsorbent were lower. It suggests that the CS/PEG/PAA adsorbent has a good reusability and is a promising candidate for practical application in wastewater treatment. The increased adsorption capacity of Pb^{2+} can be ascribed to several reasons; i.e., (i) EDTA-4Na activates new adsorption sites, and (ii) new adsorption sites prefer adsorption of Pb^{2+}.

Figure 10 shows the kinetics of the fourth desorption of Pb^{2+} and Cd^{2+} from the CS/PEG/PAA adsorbent. The desorption capacity of Pb^{2+} and Cd^{2+} ions increased with contact time until it reached equilibrium after 120 min. It indicated that the desorption of Pb^{2+} and Cd^{2+} ions using EDTA-4Na as eluent is a slow process compared with the adsorption process. The equilibrium desorption capacities of Pb^{2+} and Cd^{2+} ions are 495.0 and 201.7 mg g^{-1}, respectively.

In order to evaluate the desorption behavior, the pseudo-first-order and pseudo-second-order desorption kinetic equations were used to investigate the experimental data, which were given as follows:

$$\log\left(Q_{e,d}-Q_{t,d}\right) = \log Q_{e,d} - \frac{k_{1,d}}{2.303}t \tag{8}$$

$$\frac{t}{Q_{t,d}} = \frac{1}{k_{2,d}Q_{e,d}^2} + \frac{t}{Q_{e,d}} \tag{9}$$

where $Q_{e,d}$ (mg g^{-1}) and $Q_{t,d}$ (mg g^{-1}) are the desorption capacities at equilibrium and time t. $k_{1,d}$ (min^{-1}) and $k_{2,d}$ (g mg^{-1} min^{-1}) are the desorption rate constants of the pseudo-first order and pseudo-second order.

Figure 11 shows the pseudo-first-order kinetic model (Fig. 11a) and pseudo-second-order kinetic model (Fig. 11b) of desorption. The kinetic parameters of desorption are listed in Table 5. Compared with the pseudo-first-order kinetic parameters, the R^2 values of the pseudo-second-order kinetic model are closer to 1. Meanwhile, the $Q_{e,d}$ values are slightly different from the experimental data $Q_{e,d,exp}$. It indicated that the desorption processes of Pb^{2+} and Cd^{2+} on CS/PEG/PAA adsorbent all obey the pseudo-second-order kinetic desorption model. So, the rate-limiting step of desorption is a chemical process. That is, the adsorption and desorption processes fit the same type of kinetic behavior. A similar result was reported for desorption of Cu^{2+} from magnetic polymer adsorbent by Tseng et al. [38]. By comparing the k_2 (Table 1) and $k_{2,d}$ (Table 5) of Pb^{2+} and Cd^{2+}, it indicated that the desorption of Pb^{2+} and Cd^{2+} ions using 0.015 mol L^{-1} EDTA-4Na as eluent was a slow process.

Table 5 Kinetic parameters for desorption of Pb^{2+} and Cd^{2+} using 0.015 mol L^{-1} EDTA-4Na as eluent

Metal ions	$Q_{e,d,exp.}$ (mg g^{-1})	Pseudo-first-order model			Pseudo-second-order model		
		$k_{1,d}$ (min^{-1})	$Q_{e,d}$ (mg g^{-1})	R^2	$k_{2,d} \times 10^{-4}$ (g mg^{-1} min^{-1})	$Q_{e,d}$ (mg g^{-1})	R^2
Pb^{2+}	495.0	0.041	324.2	0.9408	2.89	515.5	0.9998
Cd^{2+}	201.7	0.038	152.6	0.9816	4.73	214.6	0.9995

Conclusion

Chitosan/poly(ethylene glycol)/poly(acrylic acid) (CS/PEG/PAA) adsorbent prepared by glow-discharge electrolysis plasma (GDEP) was successfully employed to remove Pb^{2+} and Cd^{2+} from aqueous solution. Copolymerization mechanism initiated by GDEP is a free radical addition-crosslinking reaction. FT-IR analysis revealed that PEG and AA have been grafted onto the CS backbone. TG/DTG suggested that grafted PEG and AA onto CS can improve the thermal stability of the CS. SEM showed that the adsorbent has a rough surface and a network structure with many pores. The optimum pH of Pb^{2+} and Cd^{2+} adsorption is pH 4.8, and the adsorption equilibrium is 60 min. The equilibrium adsorption capacities of CS/PEG/PAA adsorbent for Pb^{2+} and Cd^{2+} at pH 4.8 with 25 °C are 431.7 and 265.0 mg g^{-1}, respectively. Adsorption kinetics of single and binary components on adsorbent fit well the pseudo-second-order model. The CS/PEG/PAA absorbent has a good selectivity for Pb^{2+} with the coexistence of Cd^{2+}. After regeneration for four times, the adsorption capacities are still high and have no noticeable change compared with the first time using EDTA-4Na as eluent. The fourth desorption kinetics follows the pseudo-second-order model. All the results indicated that CS/PEG/PAA adsorbent has large adsorption capacities, promising reusability, and high selectivity for Pb^{2+}. It can be used as a very promising absorbent for the separation, purification, and selective recovery of Pb^{2+} in aqueous systems. This study also shows that using GDEP as initiation to fabricate CS/PEG/PAA absorbent is an effective strategy for the development of high-performance absorbent.

Acknowledgments This work was supported in part by the National Natural Science Foundation of China (No. 21367023, 21567025, and 11564037) and Natural Science Foundation of Gansu Province (No. 1308RJZA144), China.

Compliance with ethical standards

Conflict of interest The authors declare that they have no competing interests.

References

1. Meena AK, Mishra GK, Rai PK, Rajagopal C, Nagar PN (2005) Removal of heavy metal ions from aqueous solutions using carbon aerogel as an adsorbent. J Hazard Mater B 122:61–170. doi:10.1016/j.jhazmat.2005.03.024
2. Liu YM, Ju XJ, Xin Y, Zheng WC, Wang W, Wei J, Xie R, Liu Z, Chu LY (2014) A novel smart microsphere with magnetic core and ion-recognizable shell for Pb^{2+} adsorption and separation. ACS Appl Mater Interfaces 6:9530–9542. doi:10.1021/am501919j
3. Li X, Li Y, Ye Z (2011) Preparation of macroporous bead adsorbents based on poly(vinyl alcohol)/chitosan and their adsorption properties for heavy metals from aqueous solution. Chem Eng J 178:60–68. doi:10.1016/j.cej.2011.10.012
4. Gandhi MR, Meenakshi S (2012) Preparation and characterization of silica gel/chitosan composite for the removal of Cu(II) and Pb(II). Int J Biol Macromol 50:650–657. doi:10.1016/j.ijbiomac.2012.01.012
5. Laus R, Costa TG, Szpoganicz B, Fávere VT (2010) Adsorption and desorption of Cu(II), Cd(II) and Pb(II) ions using chitosan crosslinked with epichlorohydrin-triphosphate as the adsorbent. J Hazard Mater 183:233–241. doi:10.1016/j.jhazmat.2010.07.016
6. Zhou G, Luo J, Liu C, Chu L, Ma J, Tang Y, Zeng Z, Luo S (2016) A highly efficient polyampholyte hydrogel sorbent based fixed-bed process for heavy metal removal in actual industrial effluent. Water Res 89:151–160. doi:10.1016/j.watres.2015.11.053
7. Yu J, Li Y, Lu QF, Zheng JD, Yang SX, Jin F, Wang QZ, Yang W (2016) Synthesis, characterization and adsorption of cationic dyes by CS/P(AMPS-co-AM) hydrogel initiated by glow-discharge-electrolysis plasma. Iran Polym J 25:423–435. doi:10.1007/s13726-016-0434-8
8. Yu J, Zhang HT, Li Y, Lu QF, Wang QZ, Yang W (2016) Synthesis, characterization, and property testing of PGS/P(AMPS-co-AM) superabsorbent hydrogel initiated by glow-discharge electrolysis plasma. Colloid Polym Sci 294:257–270. doi:10.1007/s00396-015-3751-0
9. Guibal E (2004) Interactions of metal ions with chitosan-based sorbents: a review. Sep Purif Technol 38:43–74. doi:10.1016/j.seppur.2003.10.004
10. Wu FC, Tseng RL, Juang RS (2010) A review and experimental verification of using chitosan and its derivatives as adsorbents for selected heavy metals. J Environ Manag 91:798–806. doi:10.1016/j.jenvman.2009.10.018
11. Zhao F, Repo E, Sillanpää M, Meng Y, Yin D, Tang WZ (2015) Green synthesis of magnetic EDTA- and/or DTPA-cross-linked chitosan adsorbents for highly efficient removal of metals. Ind Eng Chem Res 54:1271–1281. doi:10.1021/ie503874x
12. Paulino AT, Belfiore LA, Kubota LT, Munizd EC, Almeida VC, Tambourgi EB (2011) Effect of magnetite on the adsorption behavior of Pb(II), Cd(II), and Cu(II) in chitosan-based hydrogels. Desalination 275:187–196. doi:10.1016/j.desal.2011.02.056
13. Kyzas GZ, Siafaka PI, Lambropoulou DA, Lazaridis NK, Bikiaris DN (2014) Poly(itaconic acid)-grafted chitosan adsorbents with different cross-linking for Pb(II) and Cd(II) uptake. Langmuir 30:120–131. doi:10.1021/la402778x
14. Zhao F, Repo E, Yin D, Sillanpää M (2013) Adsorption of Cd(II) and Pb(II) by a novel EGTA-modified chitosan material: kinetics and isotherms. J Colloid Interface Sci 409:174–182. doi:10.1016/j.jcis.2013.07.062
15. Khan A, Badshah S, Airoldi C (2011) Biosorption of some toxic metal ions by chitosan modified with glycidylmethacrylate and diethylenetriamine. Chem Eng J 171:159–166. doi:10.1016/j.cej.2011.03.081
16. Aliabadi M, Irani M, Ismaeili J, Piri H, Parnian MJ (2013) Electrospun nanofiber membrane of PEO/chitosan for the adsorption of nickel, cadmium, lead and copper ions from aqueous solution. Chem Eng J 220:237–243. doi:10.1016/j.cej.2013.01.021
17. Nguyen NT, Liu JH (2013) Fabrication and characterization of poly(vinyl alcohol)/chitosan hydrogel thin films via UV irradiation. Eur Polym J 49:4201–4211. doi:10.1016/j.eurpolymj.2013.09.032
18. Gad YH (2008) Preparation and characterization of poly(2-acrylamido-2-methylpropanesulfonic acid)/chitosan hydrogel using gamma irradiation and its application in wastewater treatment. Radiat Phys Chem 77:1101–1107. doi:10.1016/j.radphyschem.2008.05.002

19. Malik MA, Ghaffar A, Malik SA (2001) Water purification by electrical discharges. Plasma Sources Sci Technol 10:82–91. doi:10.1088/0963-0252/10/1/311
20. Lu QF, Yu J, Gao JZ, Yang W, Li Y (2012) A promising absorbent of acrylic acid/poly(ethylene glycol) hydrogel prepared by glow-discharge electrolysis plasma. Cent Eur J Chem 10:1349–1359. doi:10.2478/s11532-012-0055-9
21. Lu QF, Yu J, Gao JZ, Yang W, Li Y (2011) Glow-discharge electrolysis plasma induced synthesis of polyvinylpyrrolidone/acrylic acid hydrogel and its adsorption properties for heavy-metal ions. Plasma Process Polym 8:803–814. doi:10.1002/ppap.201000144
22. Yu J, Yang GG, Pan YP, Lu QF, Yang W, Gao JZ (2014) Poly(acrylamide-co-acrylic acid) hydrogel induced by glow-discharge electrolysis plasma and its adsorption properties for cationic dyes. Plasma Sci Technol 16:767–776. doi:10.1088/1009-0630/16/8/07
23. Liu C, Bai R (2010) Extended study of DETA-functionalized PGMA adsorbent in the selective adsorption behaviors and mechanisms for heavy metal ions of Cu, Co, Ni, Zn, and Cd. J Colloid Interface Sci 350:282–289. doi:10.1016/j.jcis.2010.04.084
24. Yantasee W, Lin Y, Fryxell GE, Alford KL, Busche BJ, Johnson CD (2004) Selective removal of copper(II) from aqueous solutions using fine-grained activated carbon functionalized with amine. Ind Eng Chem Res 43:2759–2764. doi:10.1021/ie030182g
25. Koong LF, Lam KF, Barford J, McKay G (2013) A comparative study on selective adsorption of metal ions using aminated adsorbents. J Colloid Interface Sci 395:230–240. doi:10.1016/j.jcis.2012.12.047
26. Li Z, Xiao D, Ge Y, Koehler S (2015) Surface-functionalized porous lignin for fast and efficient lead removal from aqueous solution. ACS Appl Mater Interfaces 7:15000–15009. doi:10.1021/acsami.5b03994
27. Irving H, Williams RJP (1953) The stability of transition-metal complexes. J Chem Soc 8:3192–3210. doi:10.1039/JR9530003192
28. Pearson RG (1963) Hard and soft acids and bases. J Am Chem Soc 85:3533–3539. doi:10.1021/ja00905a001
29. Pearson RG (1968) Hard and soft acids and bases, HSAB, part 1: fundamental principles. J Chem Educ 45:581–587. doi:10.1021/ed045p581
30. Şengil İA, Özacar M (2009) Competitive biosorption of Pb^{2+}, Cu^{2+} and Zn^{2+} ions from aqueous solutions onto valonia tannin resin. J Hazard Mater 166:1488–1494. doi:10.1016/j.jhazmat.2008.12.071
31. Lam KF, Yeung KL, McKay G (2006) A rational approach in the design of selective mesoporous adsorbents. Langmuir 22:9632–9641. doi:10.1021/la061410p
32. Li K, Wang Y, Huang M, Yan H, Yang H, Xiao S, Li A (2015) Preparation of chitosan-graft-polyacrylamide magnetic composite microspheres for enhanced selective removal of mercury ions from water. J Colloid Interface Sci 455:261–270. doi:10.1016/j.jcis.2015.05.043
33. Chen X, Lam KF, Mak SF, Yeung KL (2011) Precious metal recovery by selective adsorption using biosorbents. J Hazard Mater 186:902–910. doi:10.1016/j.jhazmat.2010.11.088
34. Beisebekov MM, Serikpayeva SB, Zhumagalieva SN, Beisebekov MK, Abilov ZA, Kosmella S, Koetz J (2015) Interactions of bentonite clay in composite gels of non-ionic polymers with cationic surfactants and heavy metal ions. Colloid Polym Sci 293:633–639. doi:10.1007/s00396-014-3463-x
35. Song X, Li C, Xu R, Wang K (2012) Molecular-ion-imprinted chitosan hydrogels for the selective adsorption of silver(I) in aqueous solution. Ind Eng Chem Res 51:11261–11265. doi:10.1021/ie3010989
36. Heidari A, Younesi H, Mehraban Z, Heikkinen H (2013) Selective adsorption of Pb(II), Cd(II), and Ni(II) ions from aqueous solution using chitosan-MAA nanoparticles. Int J Biol Macromol 61:251–263. doi:10.1016/j.ijbiomac
37. Li YH, Di Z, Ding J, Wu D, Luan Z, Zhu Y (2005) Adsorption thermodynamic, kinetic and desorption studies of Pb^{2+} on carbon nanotubes. Water Res 39:605–609. doi:10.1016/j.watres.2004.11.004
38. Tseng JY, Chang CY, Chang CF, Chen YH, Chang CC, Ji DR, Chiu CY, Chiang PC (2009) Kinetics and equilibrium of desorption removal of copper from magnetic polymer adsorbent. J Hazard Mater 171:370–377. doi:10.1016/j.jhazmat.2009.06.030
39. Joshi AA, Locke BR, Arce P, Finney WC (1995) Formation of hydroxyl radicals, hydrogen peroxide and aqueous electrons by pulsed streamer corona discharge in aqueous solution. J Hazard Mater 41:3–30. doi:10.1016/0304-3894(94)00099-3
40. Brisset JL, Moussa D, Doubla A, Hnatiuc E, Hnatiuc B, Youbi GK, Herry JM, Naïtali M, Bellon-Fontaine MN (2008) Chemical reactivity of discharges and temporal post-discharges in plasma treatment of aqueous media: examples of gliding discharge treated solutions. Ind Eng Chem Res 47:5761–5781. doi:10.1021/ie701759y
41. Joshi RP, Thagard SM (2013) Streamer-like electrical discharges in water: part II. Environmental applications. Plasma Chem Plasma Process 33:17–49. doi:10.1007/s11090-013-9436-x
42. Sun B, Sato M, Clements JS (1997) Optical study of active species produced by a pulsed streamer corona discharge in water. J Electrost 39:189–202. doi:10.1016/S0304-3886(97)00002-8
43. Baerdemaeker FD, Šimek M, Schmidt J, Leys C (2007) Characteristics of ac capillary discharge produced in electrically conductive water solution. Plasma Sources Sci Technol 16:341–354. doi:10.1088/0963-0252/16/2/018
44. Lukeš, P (2001) Water treatment by pulsed streamer corona discharge. PhD Thesis, Institute of Chemical Technology, Prague, Czech Republic
45. Jiang B, Zheng JT, Qiu S, Wu MB, Zhang QH, Yan ZF, Xue QZ (2014) Review on electrical discharge plasma technology for wastewater remediation. Chem Eng J 236:348–368. doi:10.1016/j.cej.2013.09.090
46. Neto CGT, Giacometti JA, Job AE, Ferreira FC, Fonseca JLC, Pereira MR (2005) Thermal analysis of chitosan based networks. Carbohydr Polym 62:97–103. doi:10.1016/j.carbpol.2005.02.022
47. Kyzas GZ, Siafaka PI, Pavlidou EG, Chrissafis KJ, Bikiaris DN (2015) Synthesis and adsorption application of succinyl-grafted chitosan for the simultaneous removal of zinc and cationic dye from binary hazardous mixtures. Chem Eng J 259:438–448. doi:10.1016/j.cej.2014.08.019
48. Zeng G, Pang Y, Zeng Z, Tang L, Zhang Y, Liu Y, Zhang J, Lei X, Li Z, Xiong Y, Xie G (2012) Removal and recovery of Zn^{2+} and Pb^{2+} by imine-functionalized magnetic nanoparticles with tunable selectivity. Langmuir 28:468–473. doi:10.1021/la203810c
49. He J, Lu Y, Luo G (2014) Ca(II) imprinted chitosan microspheres: an effective and green adsorbent for the removal of Cu(II), Cd(II) and Pb(II) from aqueous solutions. Chem Eng J 244:202–208. doi:10.1016/j.cej.2014.01.096
50. Dragan ES, Cocarta AI, Dinu MV (2014) Facile fabrication of chitosan/poly(vinyl amine) composite beads with enhanced sorption of Cu^{2+}. Equilibrium, kinetics, and thermodynamics. Chem Eng J 255:659–669. doi:10.1016/j.cej.2014.06.098
51. Lu Y, He J, Luo G (2013) An improved synthesis of chitosan bead for Pb(II) adsorption. Chem Eng J 226:271–278. doi:10.1016/j.cej.2013.04.078
52. Xiao X, Hayashi F, Shiiba H, Selcuk S, Ishihara K, Namiki K, Shao L, Nishikiori H, Selloni A, Teshim K (2016) Platy $KTiNbO_5$ as a selective Sr ion adsorbent: crystal growth, adsorption experiments, and DFT calculations. J Phys Chem C 120:11984–11992. doi:10.1021/acs.jpcc.6b02422
53. Chen CY, Chen SY (2004) Adsorption properties of a chelating resin containing hydroxy group and iminodiacetic acid for copper ions. J Appl Polym Sci 94:2123–2130. doi:10.1002/app.21079